【Memoirs of Construction Engineering Research Institute Vol.65(papers)Nov.2023】

EVALUATION OF UNSATURATED SLOPE STABILITY UNDER RAINFALL INFILTRATION

Depu Hu, Shoji Kato and Byeong-Su Kim

ABSTRACT

Rainwater infiltration is a primary cause of slope failure and studying the behavior of unsaturated slopes subjected to wet-dry cycles is of paramount importance. In this study, the stability of infinite slopes subjected to hydraulic hysteresis during wet-dry cycles using three typical soils: Toyoura sand, Hiroshimado soil, and DL clay is evaluated. Initially, the soil water characteristic curves (SWCC) as well as the suction stress characteristic curves (SSCC) of these soils were analyzed. The study then factored in the role of suction stress as confining pressure to assess the factor of safety (FOS) under both wet and dry conditions. The results suggest that the effect of suction stress acting as confining pressure exhibits the peak when the suction matches the air-entry value (AEV). However, as one moves deeper from the slope surface, the difference between the wetting FOS and drying FOS diminishes rapidly. In contrast, for soils with high cohesion, the influence of hydraulic hysteresis is minimal. Consequently, using only the drying process performance to assess the entire wet-dry cycle may underestimate the risk for failure, especially in the case of shallow failures.

1. INTRODUCTION

Japan, an island nation, consists of four main islands. Approximately three-quarters of its land area is mountainous, and storms are one of the most common disasters. According to the Ministry of Land[1], soil disasters surpass 1,000 cases annually. In 2019, this number spiked to a staggering 2,000 cases. The majority of these disasters occur between June and October, a period marked by highly unstable climatic conditions. Given the prevalence of high-intensity storms, it is essential to assess the influence of rainwater infiltration on unsaturated slope disasters. This study focuses on three representative soils: Toyoura sand, Hiroshima decomposed granite soil (Masado soil), and DL clay. It aims to explore soil stability under varying rainfall conditions.

The soil-water characteristic curve (SWCC) stands as a pivotal property for unsaturated soils, denoting the relationship between soil moisture and matric suction. Typically, soil moisture increase will cause the decrease in soil suction. Yet, even under similar conditions, the same soil might exhibit variations in soil moisture for identical suction levels (Fig.1)[2]. This is evident when comparing the SWCC during the wetting process to that of the drying process, where the former consistently presents lower values, a phenomenon termed as the SWCC hysteresis. Tao et al.[3] delved into the effects of hysteresis on the SWCC across cyclic drying and wetting cycles through the vantage points of porosity and the internal friction angle. While theoretical frameworks suggest that hysteresis would invariably influence SWCC and subsequent computations, its exploration remains scant. This oversight is often attributed to constraints in computational models[4-6] and measurement methodology.

In parallel, recent studies have broached the hysteresis effect of SWCC on slope stability[7,8]. However, these investigations primarily centered around singular soil types, rendering their findings potentially skewed by specific soil

properties and thus not universally applicable. A salient factor in these studies is hydraulic conductivity (κ). For a given soil, the drying process usually exhibits a higher κ value than that for the wetting process. Given consistent rainfall and time duration, the resulting soil moisture derived from drying and wetting κ curves will differ, and this discrepancy is further nuanced by the soil type in question. Therefore, the simulated factor of safety (FOS) might be inaccurately gauged. This paper seeks to dissect the variations between drying FOS and wetting FOS corresponding to identical saturation levels, sidestepping the confounding factor of hydraulic conductivity.

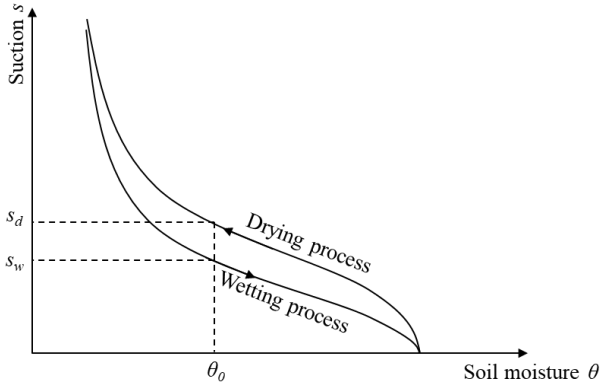

Fig.1 Hysteresis of the SWCC

2. CALCULATION MODEL

2.1 EFFECT OF SUCTION STRESS AS THE CONFINING PRESSURE

The general equations for the shear strength of unsaturated soil can be derived as the extension of effective stress (i.e., skeleton stress) equation proposed by Bishop[9]:

$$\sigma' = (\sigma - u_a) + (u_a - u_w)\chi \tag{1}$$

where σ is the total normal stress; u_a is the pore-air pressure; u_w is the pore-water pressure; $(u_a - u_w)$ is suction; $(\sigma - u_a)$ is the net stress perpendicular to the contact surface; χ is parameter related to soil saturation. On this basis, the shear strength of unsaturated soil is given through Mohr's failure criterion:

$$\tau = c' + (\sigma - u_a)\tan\varphi' + (u_a - u_w)\chi \tag{2}$$

where c' is the effective cohesion of soil; φ' is the effective angle of internal friction angle.

As mentioned above, various prediction models can be used to compute the "effective stress parameter χ" defined by Bishop[9], and the structures of formulas are generally similar. The main difference lies in the way to calculate the contribution of suction to the shear strength of unsaturated soil. This study will use the model of Vanapalli et al.[10] to calculate the shear strength of unsaturated soils:

$$\tau_f = c' + (\sigma - u_a)\tan\varphi' + (u_a - u_w) \times \left[(\tan\varphi')\left(\frac{\theta_w - \theta_r}{\theta_s - \theta_r}\right)\right] \tag{3}$$

where θ_w is the current volumetric water content; θ_r is the residual volumetric water content. θ_s is the saturated volumetric water content.

This model can well capture the altering characteristics of the shear strength when the volumetric water content or saturation varies. However, it cannot simulate the altering state of shear stress well when the water content exceeds the residual zone (θ_w<θ_r). For this study, the key point is the impact of changes in soil water moisture on shear strength, and the SWCC hysteresis effect does not involve the situation where the soil reaches the residual state and continues to lose water. Therefore, the model is available to predict the soil performance with the moisture changes. On this basis, Karube and Kato[11] summarized the contribution of suction to shear strength as suction stress. As shown:

$$p_s = S_e * s = \frac{\theta_w - \theta_r}{\theta_s - \theta_r} * s = \frac{S - Sr}{100 - Sr} * s \tag{4}$$

where p_s is the suction stress; S_e is the effective saturation; $s = u_a - u_w$ is the suction. S is the current degree of saturation; Sr is the residual degree of saturation.

On this basis, Kato et al.[12] experimentally concluded that the suction stress (p_s) in unsaturated soil can also be considered as the part of the confining pressure to further increase the shear strength rather than only acting as the cohesion component (c').

In detailly, if the calculation is conducted according to Eq. (3), the suction stress will be only considered as a part of the cohesion. In this case, when performing the unconfined compression test on the unsaturated soil, the Mohr's circle should be tangent to the Y axis (like unconfined compression test for saturated soil in Fig.2a). However, according to Kato et al.[12] experiment results of the unconfined compression test on unsaturated soil, the distance appears between the experimentally obtained Mohr's circle and the Y axis (Fig.2b). And Kim et al.[13] proved that this distance is exactly equal to the suction stress (p_s) through geometric methods.

Therefore, it can be considered that the p_s in unsaturated soil effects not only on a part of the cohesion, but also contributes to the shear strength as a part of the confining pressure, which is recognized under low confining pressure condition. Then the formula can be modified as:

$$\tau_f = c' + (\sigma - u_a + p_s)\tan\varphi' + (u_a - u_w)\left[(\tan\varphi')\left(\frac{S - S_r}{100 - S_r}\right)\right] \tag{5}$$

However, the contribution of suction stress to the FOS has rarely been studied. Therefore, under the condition of p_s acting as confining pressure, the influence of wet-dry cycle on FOS deserves further discussion.

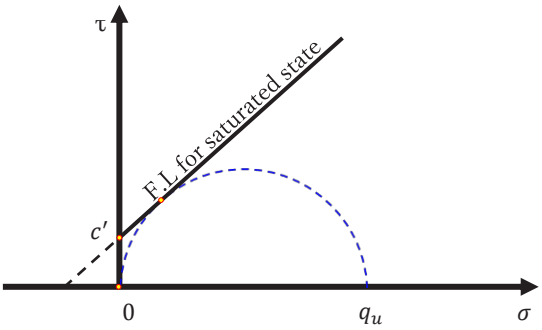

Fig.2a Unconfined compression test for saturated soil

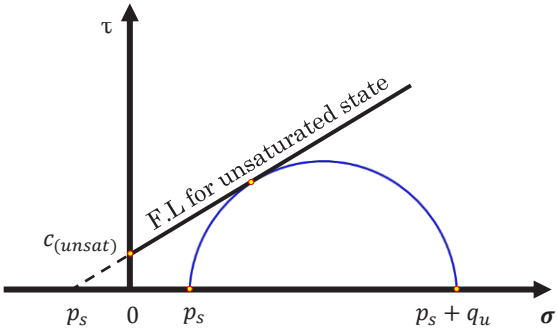

Fig.2b Unconfined compression test for unsaturated soil

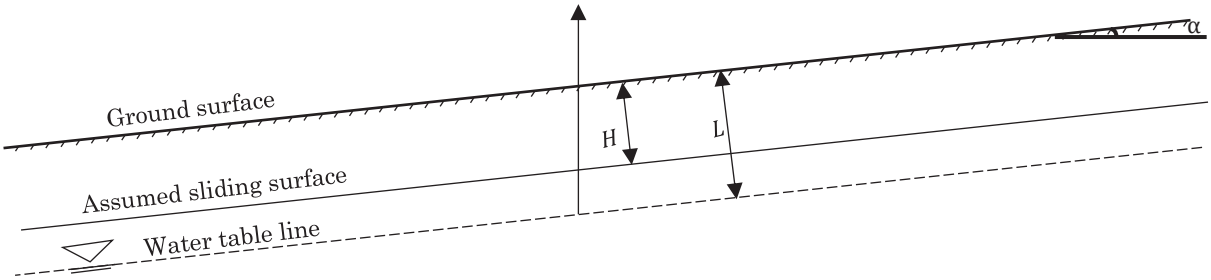

Fig.3 Diagram of an infinite slope

2.2 FACTOR OF SAFETY OF UNSATURATED INFINITE SLOPE

This paper will analyze the assumed homogeneous infinite unsaturated slope (Fig. 3). When the sliding surface is in the soil layer with depth H, its FOS can be expressed as[14]:

$$F_s = \frac{c_s + (\sigma - u_a)\tan\varphi'}{\gamma_t H \sin\alpha} \tag{6}$$

where F_s is the safety factor; c_s is the total cohesion of soil, including cohesion of saturated part c' and the contribution of suction stress to cohesion $(p_s \tan\varphi')$ in the unsaturated part; γ_t is the volumetric weight of the soil; H is the depth of sliding surface below the ground surface; α is the angle of the slope. Then, as described in Eq. (3), since there is another suction stress as an additional confining pressure, the formula is transformed into:

$$F_s = \frac{c_s + (\sigma - u_a + p_s)\tan\varphi'}{\gamma_t H \sin\alpha} \tag{7}$$

And for the theoretically infinite slope, the mutual forces between the slices can be ignored, and the normal stress perpendicular to the slope all comes from the component of gravity, that is:

$$\sigma - u_a = \gamma_t H \cos\alpha \tag{8}$$

Therefore, Eq. (7) can be rewritten as:

$$F_s = \frac{c_s}{\gamma_t H \sin\alpha} + \frac{\tan\varphi'}{\tan\alpha} + \frac{p_s \tan\varphi'}{\gamma_t H \sin\alpha} \tag{9}$$

2.3 ANALYSIS OF LIMIT EQUILIBRIUM STATE

For the conduction of the theoretical evaluation on general finite slope, the force analysis in the limit equilibrium state is the popular methods, and the corresponding safety factor can be computed according to the force equilibrium or moment equilibrium. Compared with the formula calculation method of Cho and Lee[14], it has a higher degree of flexibility. Since the limit equilibrium analysis method is not an assumed infinite slope, the required number of soil slices can be adjusted according to the actual slope size. However, due to its complex calculation, computer software is usually used for the process.

Traditionally, flow net was one of the most commonly approach to solve seepage problems. However, the construction of flow net is not a trivial task. This study will use SEEP/W and SLOPE/W in Geostudio to perform accurate seepage numerical analyzes[15,16]. For analysis of rainfall penetration problems through SEEP/W, slope geometry, boundary conditions, and parameters for SWCC, soil material, and hydraulic conductivity are required. In the simulation of slope behavior under rainwater infiltration, as an input boundary condition, flux could be controlled on the slope surface. When rainfall occurs, runoff is simulated with the provision of zero constant water pressures to slope surface. And SEEP/ W outputs the distribution of pore-water pressure at different position points and time points. Further, Limit equilibrium method is used in SLOPE/W to determine the FOS, then find the critical slip surface and the minimum FOS with time. The basic calculation logic is as follows:

According to the definition of FOS: $F = \tau_f/\tau$, the reduced shear strength of soil slice (mobilized shear force) can be given as:

$$\tau_m = \frac{\beta\tau_f}{F} = \frac{\beta}{F}[c_s + (\sigma - u_a + p_s)\tan\varphi'] \tag{10}$$

where, τ_m is the mobilized shear stress; τ_f is the shear strength; τ is the shear stress; F is the factor of safety; β is the projection of the width of the soil slice on the bottom of the slip surface. $\sigma_n = \frac{N}{\beta}$ is the average normal stress perpendicular to the sliding surface. Therefore, the equilibrium equation of each soil slice can be written according to the moment equilibrium and force equilibrium respectively:

Taking the circle center of the sliding surface as the reference for moment equilibrium:

$$Wx_W + E_L x_{E_L} - E_R x_{E_R} + X_L x_{X_L} - X_R x_{X_R} - \tau_m x_{\tau_m} - N x_N = 0 \tag{11}$$

Force equilibrium in the horizontal direction:

$$E_L - E_R - \tau_m \cos\alpha - N \sin\alpha = 0 \tag{12}$$

where: W is the self-weight of each soil slice; N is the normal force on the base of the slice; x_i is the distance from each force to the circle center of the slip surface; E_L, E_R, X_L, X_R are the horizontal compression force and vertical shear force caused by the soil slices adjacent to the selected soil slice, noting that the mark "L" and "R" stand for left and right, respectively. However, this is only the force situation of one soil slice. Since all soil slices need to be summed in subsequent calculations, the forces E and X between slices can be considered as the state of mutual cancellation respectively under the condition of no external force.

Substituting Eq. (11) and Eq. (12) into Eq. (10), the two expressions of moment equilibrium and force equilibrium of safety factor can be written in the form of Eq. (13) and Eq. (14):

$$F_m = \frac{\sum \beta R[c_s + (\sigma - u_a + p_s)\tan\varphi']}{\sum W x_W - \sum N x_N} \tag{13}$$

$$F_f = \frac{\sum \beta \cos\alpha\,[c_s + (\sigma - u_a + p_s)\tan\varphi']}{\sum N \sin\alpha} \tag{14}$$

In actual cases, the shear forces X and normal stress E applied to the selected soil slice are hard to be solved, and it is necessary to adopt some other methods to indirectly calculate the average normal stress perpendicular to the contact surface (N), such as through the force balance in the vertical direction for further analysis. This research will adopt the simplified Bishop method to obtain the factor of safety. And the normal stress E and shear force X between soil slices can be ignored. Therefore, the normal stress can be considered as $N = W\cos\alpha$.

It is worth noting that if the moment equilibrium equation and force equilibrium equation are applied to the infinite slope: for Eq. (13) and Eq. (14), the "circle center" of the slip surface on an infinitely slope can be considered as a point located at infinity perpendicular to the contact surface. Therefore $x_N = 0$, and Eq. (13) and Eq. (14) are consistent with Eq. (9).

Note that Eq. (3) is used to analyze the slope stability in SEEP/W and SLOPE/W without considering the contribution that suction stress acts as the confining pressure. That, $F_m = F(s) + F(p_s)$ can be used to modify the FOS:

$$F(s) = \frac{c_s}{\gamma_t H \sin\alpha} + \frac{\tan\varphi'}{\tan\alpha} \tag{15}$$

$$F(p_s) = \frac{p_s \tan\varphi'}{\gamma_t H \sin\alpha} \tag{16}$$

where F_m is the FOS considering p_s as the confining pressure; $F(s)$ is the FOS calculated by geotechnical simulation software, Geostudio; and $F(p_s)$ is the correction value of FOS that needs to be calculated additionally.

3. SOIL PARAMETERS AND DATA PROCESSING

In this study, the selected soil objects are Toyoura sand, Masado soil, and DL clay. Hatakeyama et al.[17] carried out continuous pressurization method on the three kinds of soils to obtain the experimental soil-water characteristic curves and the soil physical parameters are shown in Table 1.

These three kinds of soil are three representative sand, clayey soil and silt respectively. The particles of Toyoura sand are relatively large in size, and the average diameter is generally around 0.2mm, which can be considered as a soil with poor water retention performance; DL clay is just the opposite that average particle size distribution (PSD) is nearly 0.01mm, and the water retention performance is much stronger than that of Toyoura sand; Masado soil is a fine-grained material with a wide PSD.

Therefore, the infinite slope composed of these three soils will be assumed and conduct the theoretically analysis to explore the influence of the wet-dry cycle on slopes constituted by different material.

The fitting parameter for SWCCs of the wetting process and drying process are calculated by extracting the result obtained by Hatakeyama[17] and using the SWCC model of Van Genuchten[4]:

$$S_e = \left\{\frac{1}{1+[a(u_a-u_w)]^n}\right\}^{1-\frac{1}{n}} \tag{17}$$

where: a and n are fitting parameters; a is approximately the reciprocal of the air entry value; n is related to the void distribution. Combined with Eq. (3), the relationship between suction and volumetric water content can be obtained:

$$\theta_w = \left\{\frac{1}{1+[a(u_a-u_w)]^n}\right\}^{1-\frac{1}{n}} * (\theta_s-\theta_r)+\theta_r \tag{18}$$

The fitting result of SWCC are shown in Fig.4. The suction stress characteristic curve (SSCC), that is, the relationship between suction stress (p_s) and suction[18,19] are shown in Fig.5. The fitted parameters results are shown in Table 1.

Table 1 parameters of soils

Tested soils	Particles Density (g/cm^3)	Uniformity Coefficient U_c	Mean Grain Diameter $D_{50}(mm)$	$\rho_d\ (g/cm^3)$	$a_d\ (kPa)$	$a_w\ (kPa)$	n_d	n_w
Toyoura sand	2.641	1.49	0.172	1.5	0.25	0.44	5	4.1
Masado soil	2.614	46.1	0.484	1.08	2.6	5.12	1.8	1.6
DL clay	2.651	4.58	0.0171	1.5	0.03	0.04	2.33	2.36

Note: a_d, n_d, a_w, n_w *are the fitted parameter of drying process and wetting process, respectively.*

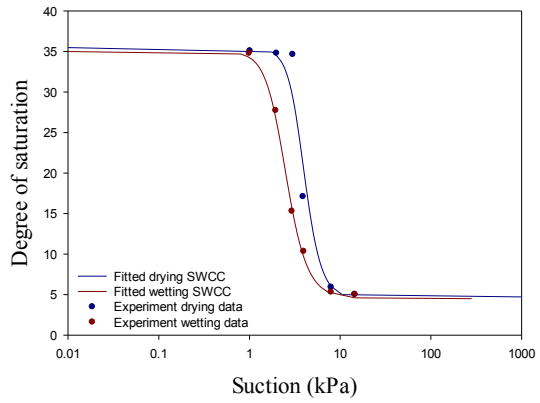

Fig.4a Fitting SWCC for Toyoura sand

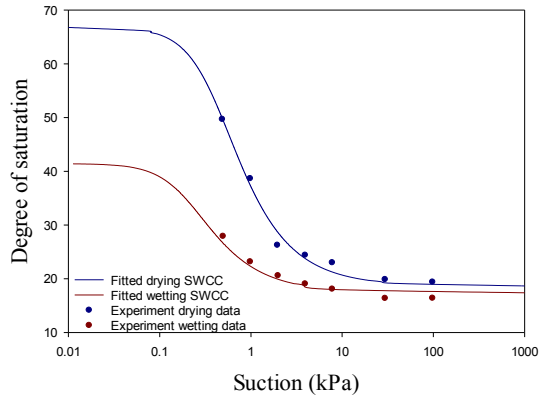

Fig.4b Fitting SWCC for Masado soil

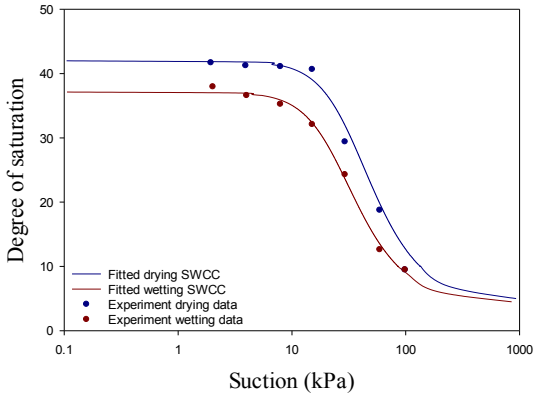

Fig.4c Fitting SWCC for DL clay

4. RESULT AND DISCUSSION

The manual calculation for the factor of safety of the homogeneous two-dimensional infinite slope will be conducted firstly. Set the distance between the selected slip surface and the ground surface denoted as H. And the soil parameters of the slope are the same as mentioned above. Then compare the results of the four cases in Table 2: Case 1: consider suction stress p_s only acts as cohesion in drying process; Case 2: consider suction stress p_s only acts as cohesion in wetting process; Case 3: consider p_s contributing to both cohesion and confining pressure in drying process; Case 4: consider p_s contributing to both cohesion and confining pressure in wetting process.

Table 2 Marks for different cases

	p_s only acts as cohesion (Eq.3)	p_s contributes to confining pressure (Eq.5)
Drying SWCC	CASE 1	CASE 3
Wetting SWCC	CASE 2	CASE 4

4.1 EFFECT OF SUCTION STRESS ON FOS

The example (Fig.3) is to examine the theoretical infinite slope under the influence of different factors. Here, to explore the behavior of shallow slopes firstly, the distance between the selected slip surface and the ground surface was set to 1 meter; The angle of inclination of slope is set to 26°; Eq. (6) and Eq. (7) are used to calculate the FOSs in the case 1,2 and case 3,4 in Table 2, respectively. The plotted profiles are shown in Fig.5.

The trend of the relationship curves between FOS and suction is almost identical to SSCCs for all 3 soils, indicating that the suction stress plays a crucial role in the FOS. For the soils with narrow PSD such as Toyoura sand and DL clay, without considering suction stress as confining pressure, the gap between FOS_{case1} and FOS_{case2} will increase with an increase in suction initially, then followed by a decrease after the suction being greater than AEV. Moreover, since the Eq. (7) adding another suction stress as the confining pressure based on the Eq. (6), the gap caused by hysteresis (between FOS_{case3} and FOS_{case4}) will further increase with the consideration of p_s acting as confining pressure. The stress corresponding to AEV can be considered as the critical value where the impact of hysteresis peaks. For the clay such as Masado soil, on the other hand, FOSs of each case will remain constant as the suction is greater than AEV, and the critical value of FOS or suction stress could be determined when suction is greater than AEV. Specifically, without considering suction stress as confining pressure, the peak of gap between FOS_{case1} and FOS_{case2} for Toyoura sand and DL clay are 0.1 and 1.1, respectively. As adds the suction stress as the confining pressure, the gaps (between FOS_{case3} and FOS_{case4}) will increase to 0.3 and 1.6 respectively. For Masado soil, however, even the maximum gap between FOS_{case3} and FOS_{case4} is less than 0.1.

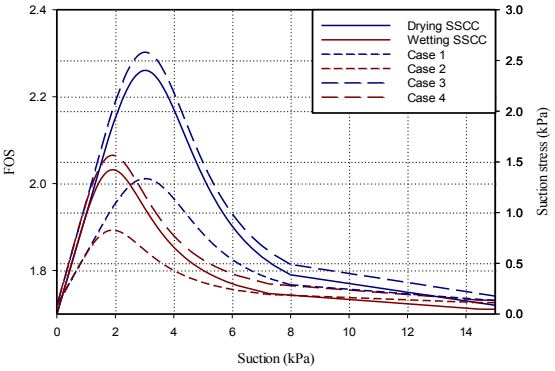

Fig.5a Relationship between FOS and suction for Toyoura sand

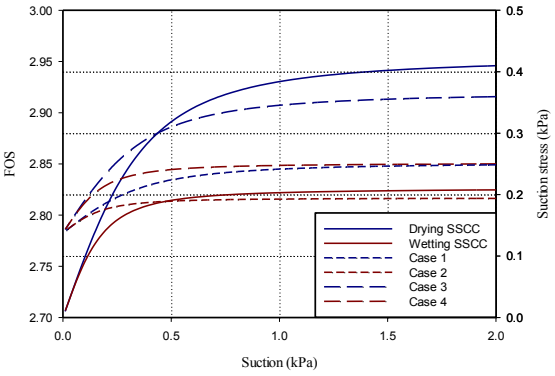

Fig.5b Relationship between FOS and suction for Masado soil

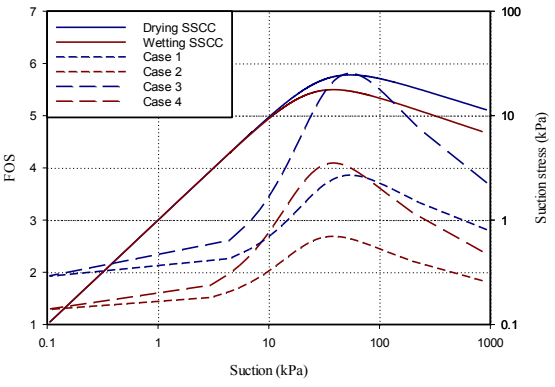

Fig.5c Relationship between FOS and suction for DL clay

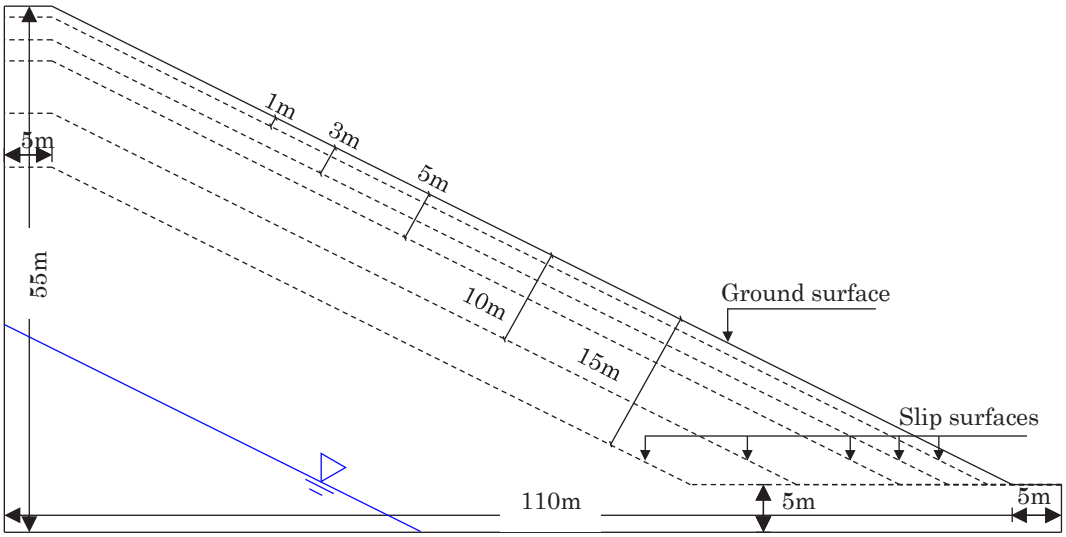

Fig.6 The model used for the simulation

Among several factors, soil properties can be considered as one of the most important factors. Due to low AEV of the selected Masado soil, which is only 0.68kPa, the suction stress of Masado soil is limited (maximum value of suction stress is only 0.4kPa). Furthermore, the cohesion (c') of masado soil is set to 5kPa in the calculation of shear strength. Therefore, compared with cohesion, the influence of the changes in suction stress on FOS is diluted. For Toyoura sand and DL clay, the cohesion is generally low, and it can be directly set to 0. Hence the influence of suction stress on FOSs is obvious. Thus, for all soils, consideration of another p_s acting as confining pressure will further amplify the impact of the hysteresis, and this amplification would be affected by soil cohesion (c').

4.2 EFFECT OF CASES ON FOS AT DIFFERENT DEPTH

To further explore the impact of SWCC hysteresis at different depths, the geotechnical simulation software, Geostudio, will be used to simulate the failure behavior of the infinite slopes. The established model is shown in Fig.6. Where the solid line in the model is the ground surface, and five dotted lines represent five cases of sliding surfaces with distances of H=1m, H=3m, H=5m, H=10m and H=15m from the ground surface, respectively. Then, the "Fully specify slip surface" command and the "Tension crack line" command can be used to make the soil slices possess the same thickness and go vertically upwards, to simulate the sliding surface of the infinite slope[16]. As hypothesis for theoretical analysis: the rainfall condition is set to be 50mm/h for 10 days, then continuous drainage for 20 days. To reduce the influence on the initial state, the water level line is set parallel to the slope and close to the bottom.

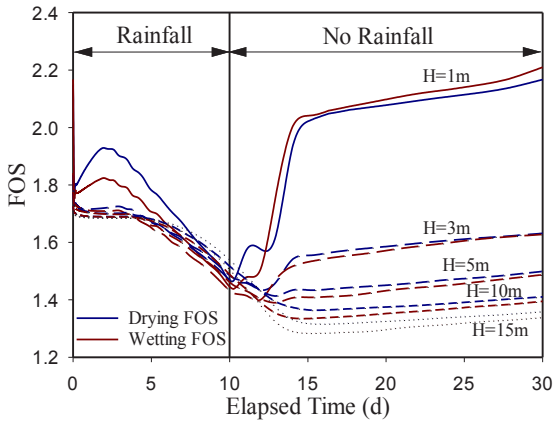

Fig.7a Relationship between FOS and time for Toyoura sand

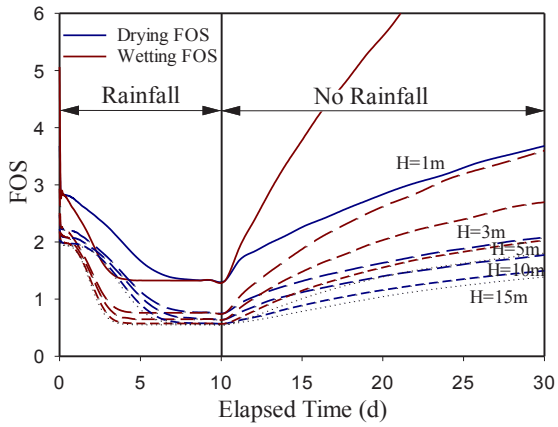

Fig.7b Relationship between FOS and time for Masado soil

Note that the study is to explore the difference of wet and dry FOS under the same water content. And for soils, generally, hydraulic conductivity (κ) in drying process (κ_d) and wetting process (κ_w) are different. It may cause different soil moisture using κ_d and κ_w even under the same rainfall infiltration. Therefore, simulation with the real soil parameter may cause greater interference. To mitigate this interference, in the simulation, the κ_d and κ_w of the same soil are set to the same constant value. Simultaneously, κ is properly tuned to adjust the rate of rainwater infiltration, so that the difference of FOSs under different cases can be observed perceptibly. Under the same rainfall conditions, the relationship curve between FOSs and elapsed time simulated through SWCC in drying process (drying SWCC) and wetting process (wetting SWCC) can be obtained (Fig. 7). Note that Eq. (13) and Eq. (14) are adopted to modify the FOS value with consideration of p_s acting as confining pressure.

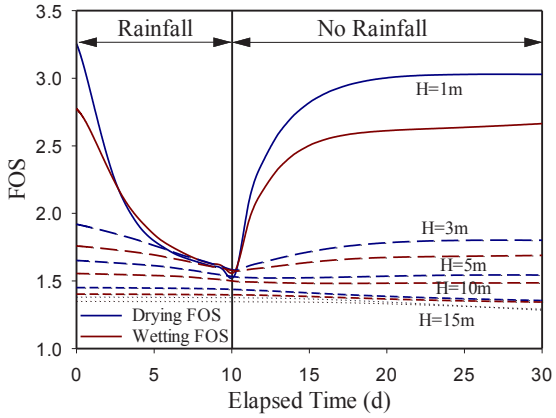

Fig.7c Relationship between FOS and time for DL clay

In terms of the relationship curve, in the rainfall stage, as the saturation increases, the FOS simulated by the wetting SWCC and drying SWCC of the three types of soils all show a decrease trend. In the wetting process, the FOS obtained from wetting SWCC (wetting FOS) is always lower than FOS obtained from drying SWCC (drying FOS), and the gap between wetting FOS and drying FOS show the decrease with an increase in soil moisture. Thus, the impact of SWCC hysteresis on the FOS is declined as the slope tends to be saturated. The results are consistent with the conclusion obtained from the theoretical calculation.

According to Fig. 7, when the sliding surface is closed to ground surface, the larger difference between the drying FOS and the wetting FOS would be observed. Specifically, when the distance between the sliding surface and the ground surface is 1m (H=1m), the maximum FOS gaps of Toyoura sand, Masado soil and DL clay are about 10%, 40% and 15%, respectively. And when the H reaches 3 meters, the gap will drastically reduce to 3%, 30% and 8%. On this basis, however, if the depth is further increased to 5m, 10m or 15m, the gaps between the drying FOS and the wetting FOS of the three soils become much less significant. Therefore, at depths greater than 5m, FOSs appear to be less sensitive to SWCC hysteresis.

5. CONCLUSION

In this paper, firstly, the influence of drying process and wetting process on soil water characteristic curve (SWCC) was analyzed. Then cited the experimental data of Toyoura sand, Masado soil and DL clay obtained by Hatakeyama et al.[17], and further examined the suction stress characteristic curve (SSCC) to analyze the influence of p_s only as cohesion and p_s as a part of confining pressure on the factor of safety (FOS), respectively. On this basis, assume the infinite slopes composed of these three soils respectively, and perform theoretical calculations. Then analyze the infinite slope stability through Geostudio simulation to verify and expand the results. The conclusions are as follow:

1. By comparing SSCCs and the relationship between FOS and suction in the infinite slope with a depth H=1m, suction stress can be considered to dominate the change of the FOS. Moreover, the disparity between FOSs calculated by wetting SWCC and by drying SWCC will further increase when p_s is considered as an extra confining pressure.
2. In addition to the particle size of soil materials, the change of FOSs will also be affected by apparent cohesion. In Masado soil, since the c' is set to 5kPa, the influence of the change of suction stress on FOS is diluted.
3. The paper use Geostudio to simulate the FOS changes of three soils at various depths. Results show that when the selected H is less than 5 m, slope stability will be greatly affected by SWCC hysteresis and p_s acting as confining pressure or not. And as the H continues to increase, this affect will be weakened rapidly.

Overall, in the previous slope stability analysis, the hysteresis effect of SWCC was usually ignored, and only the SWCC obtained from the drying process was used to estimate the soil performance in the entire process. This study verified that this method may be suitable for deep slopes. However, for shallow slopes or some specific soils, it may seriously underestimate the impact of SWCC hysteresis and p_s acting as confining pressure or only acting as apparent cohesion.

REFERENCES

1) Ministry of Land, Infrastructure, Transport and Tourism, Occurrence of sediment-related disasters in 2019, (in Japanese)
2) Rahardjo H., Heng O.B., Choon L.E., Shear strength of a compacted residual soil from consolidated drained and constant water content triaxial tests. *Canadian Geotechnical Journal*, Vol. 41(3), pp.421-436, 2004.
3) Tao G., Li Z., Liu L., Chen Y., Gu K., Effects of Contact Angle on the Hysteresis Effect of Soil-Water Characteristic Curves during Dry-Wet Cycles. *Advances in Civil Engineering*, vol. 2021(2), pp. 1-11, 2021.
4) Van Genuchten, M.Th., A closed-form equation for predicting the hydraulic conductivity of unsaturated soils. *Soil Science Society of America Journal*, Vol. 44(5), pp. 892–898, 1980.
5) Fredlund D. G., and Xing A., Equations for the soil-water characteristic curve. *Canadian Geotechnical Journal*, Vol. 31(4), pp. 521–532, 1994.
6) Brooks R. H., and Corey A. T., Hydraulic properties of porous media. *Hydrology papers (Colorado State Univ.,),* 1964.
7) Chen P., Mirus B., Lu N., Godt J.W., Effect of hydraulic hysteresis on stability of infinite slopes under steady infiltration. *J. Geo-tech. Geoenviron. Eng.* Vol. 143(9), pp. 1-10, 2017.
8) Kristo C., Rahardjo H., Satyanaga A., Effect of hysteresis on the stability of residual soil slope. Int. *Soil Water Conserv. Res*. Vol. 7(3), pp. 226–238, 2019.
9) Bishop A. W, Blight G. E., Some aspects of effective stress in saturated and partly saturated soils. *Geotechnique*, Vol. 13(3), pp. 177–97, 1963.
10) Vanapalli S. K., Fredlund D. G., Pufahl D. E., and Clifton A. W., Model for the prediction of shear strength with respect to soil suction. *Canadian Geotechnical Journal*. Vol. 33(3), pp. 379-392, 1996.
11) Karube D., Kato S., Hamada K. and Honda M., The relationship between the mechanical behavior and the state of pore water in unsaturated soil. *J. Geotech. Engrg., Proc. of JSCE*, Vol. 535, pp. 83-92, 1996 (in Japanese).
12) Kato S., Yoshimura Y., Fredlund D. G., Role of matric suction in the interpretations of unconfined compression tests. Proceedings of the 58th Canadian Geotechnical Conference, Saskatoon, SK. Vol.2, pp. 410-415, 2005.
13) Kim B. S., Park S. W., Lohani T. N., Kato S., Characterizing suction stress and shear strength for unsaturated geomaterials under various confining pressure conditions. *Transp. Geotech.* Vol. 34 (4), pp. 1-11, 2022.
14) Cho S. E., and Lee S. R., Evaluation of surficial stability for homogeneous slopes considering rainfall characteristics. *Journal of Geotechnical and Geoenvironmental Engineering*, Vol. 128 (9), pp. 756–763, 2002.
15) Geo-Slope International Ltd. (2012a). Seepage modeling with SEEP/W. Calgary, Alberta: July 2012 Edition.
16) Geo-Slope International Ltd. (2012b). Slope modeling with SLOPE/W. Calgary, Alberta: July 2012 Edition.
17) Hatakeyama M., Kyono S., and Kawahara T., Development of Water Retention Test Apparatus According to the Continuous Pressurization Method. *Oyo Technical Report*, No.34, pp.23-54, 2015 (in Japanese).
18) Kato S., Yoshimura Y., Kawai K., and Sunden W., Effects of suction on strength characteristics of unconfined compression test for a compacted silty clay. *JSCE*, Vol. 687, pp. 201-218, 2001 (in Japanese).
19) Lu N., Likos W. J., Suction stress characteristic curve for unsaturated soil. *Journal of Geotechnical and Geoenvironmental Engineering,* Vol. 132 (2), pp. 131–142, 2006.

AUTHORS

Depu Hu	Doctoral student, Graduate School of Engineering, Kobe University, Japan
Shoji Kato	Associate Prof., Dr. Eng., Graduate School of Engineering, Kobe University, Japan
Byeong-Su Kim	Associate Prof., Dr. Eng., Dept. of Civil & Environmental Eng., Dankook University, Korea